ENG TRANSACTIONS

Journal homepage: https://engtransactions.com/

ENG Transactions 4 Article ID: 2868, 1–8, December 2023

ISSN 2717-3127

Research Article

Stochastic Response Analysis of Two Vibration Systems with Impact Interactions

Yangyang Luo[1,2], Jin Yan[1,2], Dapeng Zhang[1,2*]

[1] *Ship and Maritime college, Guangdong Ocean University, Zhanjiang, China*
[2] *Shenzhen Institute of Guangdong Ocean University, Shenzhen, China*

Keywords

Vibro-impact system, Fokker-Planck-Kolmogorov method, IDFT, Stochastic Response.

Abstract

In this paper, we perform an analytic solution of a vibro-impact system including two single-degree-of-freedom vibration systems under random excitations by using the classical Fokker-Planck-Kolmogorov (FPK) method. The numerical solution of the vibro-impact systems is also performed based on the inverse discrete Fourier transform (IDFT) and the Runge-Kutta method. The mean square responses and the mean square responses ratio are calculated to study the deviation between the analytical solution and the numerical solution. Finally, the influence of clearance on the responses of the systems, such as mean square responses, contact ratio and impact force level, is discussed.

1. Introduction

Vibro-impact systems i.e. vibrating systems including impact interactions widely exist in mechanical engineering; ocean engineering and civil engineering[1-3]. Various dynamical phenomena are observed in the vibro-impact systems. For example, under deterministic periodically loadings, the stability, bifurcation and chaos of the vibro-impact system have been explored by the Poincare map [4-7]. In practice, engineering structures are often subjected to random loadings, e.g., wind load, earthquakes, ocean waves and random disturbance or noise. Due to the impact interactions and the random loadings, the vibro-impact systems are always non-smooth and nonlinear, which induces complicated system responses and imposes great challenges for proper characterization of the systems. Therefore, it is important to investigate impact interactions of the vibro-impact system under random loadings.

Various modeling techniques have been developed to study impact interactions. One widely used model is the classical impact model, which assumes that the impact process is instantaneous and uses the coefficient of restitution to modify the velocities of the colliding bodies after impact base on the principle of momentum [8]. Another model to describe the impact process is the Hertzian contact model [9], which assumes the contact force between two elastic bodies to be proportional to the 3/2 power of the relative displacement between them. However, the non-linear effects exists in both models and may lead to difficulties in solving the Fokker-Planck-Kolmogorov (FPK) equation of the vibro-impact systems, so that the exact solution for the corresponding FPK equation is known only for very few cases [10-16]. Therefore, approximate methods have been developed and employed to solve the FPK equation for obtaining the approximate probability density functions (PDFs) of the responses of the non-smooth and non-linear systems. By transforming the non-smooth systems to corresponding smooth systems, the responses of vibro-impact systems can be obtained through traditional asymptotic approaches [17].

Based on the stochastic averaging method, the approximate stationary solutions for both single-degree-of-freedom and multi-degree-of-freedom systems have been derived [18,19]. Multiple scales method has been adopted to obtain the PDFs of the responses of vibro-impact systems under different complex excitations such as external and parametric excitations, combined harmonic and random excitations [20,21]. In order to obtain the PDFs of the

* Corresponding Author: Dapeng Zhang
E-mail address: 1214265737@qq.com, ORCID: https://orcid.org/0000-0002-9525-5553

Received: 22 November 2023; Revised: 14 December 2023; Accepted: 20 December 2023
https://doi.org/10.61186/engt.4.1.2868

Academic Editor: **He Li**

Please cite this article as: Y. Luo, J. Yan, D. Zhang, Stochastic Response Analysis of Two Vibration Systems with Impact Interactions, ENG Transactions 4 (2023) 1–8, Article ID: 2868.

responses of some new strong-nonlinearity vibro-impact systems, the exponential–polynomial closure (EPC) method have been explored to solve the FPK equation of these systems [22-24].

As mentioned, most work deal with the stationary solutions of single-degree-of-freedom and multi-degree-of-freedom systems. In these work, the vibro-impact systems consist of moving oscillators and stationary barriers. However, in practice, impact between two vibration systems occurs frequently. For example, there are a great number of studies on the pounding force response spectrum between adjacent structures under earthquake excitation [25-29]. However, there are quite few studies on the stationary solutions of this composite vibro-impact system. The exact stationary solutions of the random response of two special vibration systems with impact interactions are obtained [30]. Work [30] provides useful insights into the impact interactions on the two vibration systems; however, it is lack of numerical validation. In this paper, a vibro-impact system with two single-degree-of-freedom vibration systems is considered. The contact between the two vibration systems is modeled by the Hertz law. The analytical solution of the vibro-impact system under random excitation is performed, and the numerical solution of the vibro-impact system is also presented based on the IDFT [31]. By comparing the PDFs of the displacement and velocity responses of the vibro-impact systems calculated by the two methods, the limitation of the analytical solutions is examined, and the dynamic characteristics of the systems, such as mean square responses, contact ratio and impact force level, are also discussed.

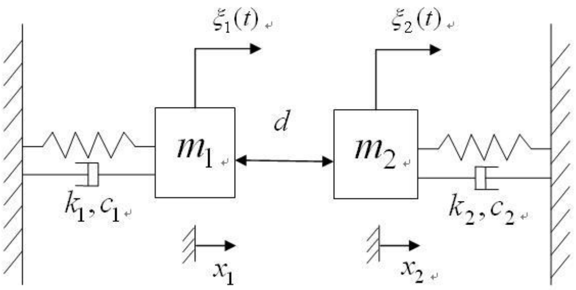

Figure 1 . Two single-degree-of-freedom vibration systems.

2. System Description and Theoretical Analysis

Consider two single-degree-of-freedom vibration systems with a clearance d placed between these two systems, as shown in Figure 1. Each system has its own mass, damping coefficient and spring constant m, c, k, and is forced by independent random excitation. The motion equations of the systems can be written as:

$$\begin{cases}\ddot{x}_1 + 2\zeta_1\omega_1\dot{x}_1 + \omega_1^2 x_1 + \eta\cdot g(x_1,x_2) = \xi_1(t) \\ \ddot{x}_2 + 2\zeta_2\omega_2\dot{x}_2 + \omega_2^2 x_2 - \eta\cdot g(x_1,x_2) = \xi_2(t)\end{cases} \tag{1}$$

where $\ddot{x}_i, \dot{x}_i, x_i, i = 1,2$ denote the accelerations, velocities and displacements of each system, respectively; $\zeta_i = \frac{c_i}{2\sqrt{m_i k_i}}$ denotes the constant damping ratios; $\omega_i = \sqrt{k_i/m_i}$ denotes the natural frequencies. η is the contact stiffness, which depends on the elastic properties and geometries of the two contacting bodies [9]. $g(x_1,x_2)$ denotes the contact force based on the Hertz law, which can be expressed as:

$$g(x_1,x_2) = \begin{cases}(x_1 - x_2 - d)^{3/2} & x_1 - x_2 - d \geq 0 \\ 0 & else\end{cases} \tag{2}$$

For simplicity, both of the random excitations $\xi_i(t)$ are assumed to be the independent stationary white Gaussian processes with zero mean. The mean and correlation function of $\xi_i(t)$ are given as below:

$$\begin{cases}E[\xi_i(t)] = 0 \qquad i = 1,2 \\ E[\xi_i(t)\xi_i(t+\tau)] = 2\pi S_i\delta(\tau) \\ E\left[\xi_i(t)\xi_j(t+\tau)\right] = 0 \quad i \neq j\end{cases} \tag{3}$$

where E denotes the expectation function, S_i denotes the spectral densities of $\xi_i(t)$, and $\delta(\tau)$ is the Dirac delta function.

Then, the joint probability density function (JPDF) $p(x_1,x_2,v_1,v_2)$ of the random responses of these systems will satisfy the stationary Fokker-Planck partial differential equation [10] , which is given as:

$$\begin{aligned}&-v_1\frac{\partial p}{\partial x_1} + \frac{\partial}{\partial v_1}\left[\left(2\zeta_1\omega_1 v_1 + \omega_1^2 x_1 + \right.\right.\\ &\left.\left.\eta g(x_1,x_2)\right)p\right] + \pi S_1\frac{\partial^2 p}{\partial v_1^2} - v_2\frac{\partial p}{\partial x_2} + \\ &\frac{\partial}{\partial v_2}\left[\left(2\zeta_2\omega_2 v_2 + \omega_2^2 x_2 - \eta g(x_1,x_2)\right)p\right] + \\ &\pi S_2\frac{\partial^2 p}{\partial v_2^2} = 0\end{aligned} \tag{4}$$

Eq. (4) can be rewritten as:

$$\begin{aligned}&\left(2\zeta_1\omega_1\frac{\partial}{\partial v_1} - \frac{\partial}{\partial x_1}\right)\left(v_1 p + \frac{\pi S_1}{2\zeta_1\omega_1}\cdot\frac{\partial p}{\partial v_1}\right) + \\ &\frac{\partial}{\partial v_1}\left[\left(\omega_1^2 x_1 + \eta g(x_1,x_2)\right)p + \frac{\pi S_1}{2\zeta_1\omega_1}\cdot\frac{\partial p}{\partial x_1}\right] + \\ &\left(2\zeta_2\omega_2\frac{\partial}{\partial v_2} - \frac{\partial}{\partial x_2}\right)\left(v_2 p + \frac{\pi S_2}{2\zeta_2\omega_2}\cdot\frac{\partial p}{\partial v_2}\right) + \\ &\frac{\partial}{\partial v_2}\left[\left(\omega_2^2 x_2 - \eta g(x_1,x_2)\right)p + \frac{\pi S_2}{2\zeta_2\omega_2}\cdot\frac{\partial p}{\partial x_2}\right] = 0\end{aligned} \tag{5}$$

One solution of Eq. (5) can be obtained if:

$$\begin{cases}v_1 p + \dfrac{\pi S_1}{2\zeta_1\omega_1}\cdot\dfrac{\partial p}{\partial v_1} = 0 \\ v_2 p + \dfrac{\pi S_2}{2\zeta_2\omega_2}\cdot\dfrac{\partial p}{\partial v_2} = 0 \\ \left(\omega_1^2 x_1 + \eta g(x_1,x_2)\right)p + \dfrac{\pi S_1}{2\zeta_1\omega_1}\cdot\dfrac{\partial p}{\partial x_1} = 0 \\ \left(\omega_2^2 x_2 - \eta g(x_1,x_2)\right)p + \dfrac{\pi S_2}{2\zeta_2\omega_2}\cdot\dfrac{\partial p}{\partial x_2} = 0\end{cases} \tag{6}$$

In order to solve Eqs.(6), we assume that (1) the displacements and velocities are statistically independent, which means

$$p(x_1,x_2,v_1,v_2) = p(x_1,x_2)p(v_1)p(v_2) \tag{7}$$

From the first and the second equations of Eqs.(6), it is found that the velocity distributions of v_1 and v_2 are still Gaussian, Thus, the expressions of $p(v_1)$ and $p(v_2)$ can be easily obtained. It should be mentioned that the joint probability density function $p(x_1, x_2)$ cannot be separated since x_1 and x_2 are coupled due to the impact interactions, which is governed by $g(x_1, x_2)$. In order to analytically solve the joint probability density function $p(x_1, x_2)$, we also assume (2) the exciting strength ratio is equal to the damping ratio of the two systems

$$\frac{S_1}{S_2} = \frac{\zeta_1 \omega_1}{\zeta_2 \omega_2} \tag{8}$$

Let $\overline{S} = S_1/S_2$, $\overline{\zeta} = \zeta_1/\zeta_2$, $\overline{\omega} = \omega_1/\omega_2$, we get a translational form of the Eq.(8):

$$\frac{\overline{S}}{\overline{\zeta} \cdot \overline{\omega}} = 1 \tag{9}$$

Then the solution of the joint probability density function $p(x_1, x_2, v_1, v_2)$ can be expressed as:

$$p(x_1, x_2, v_1, v_2) = \begin{cases} C exp\left[-\frac{v_1^2}{2\sigma_{v_1}^2} - \frac{v_2^2}{2\sigma_{v_2}^2} - \frac{x_1^2}{2\sigma_{x_1}^2} - \frac{x_2^2}{2\sigma_{x_2}^2} - \frac{2\eta(x_1 - x_2 - d)^{\frac{3}{2}}}{5\omega_1^2 \sigma_{x_1}^2}\right] \\ \quad when \quad x_1 - x_2 - d \geq 0 \\ C exp\left(-\frac{v_1^2}{2\sigma_{v_1}^2} - \frac{v_2^2}{2\sigma_{v_2}^2} - \frac{x_1^2}{2\sigma_{x_1}^2} - \frac{x_2^2}{2\sigma_{x_2}^2}\right) \quad else \end{cases} \tag{10}$$

where $\sigma_{x_i}^2 = \pi S_i / 2\zeta_i \omega_i^3$ representing the mean square response of the x_i of the corresponding linear systems, $\sigma_{v_i}^2 = \pi S_i / 2\zeta_i \omega_i$ representing the mean square response of the v_i. C is the integration constant and can be obtained by

$$\int_{-\infty}^{\infty}\int_{-\infty}^{\infty}\int_{-\infty}^{\infty}\int_{-\infty}^{\infty} p(x_1, x_2, v_1, v_2) dx_1 dx_2 dv_1 dv_2 = 1 \tag{11}$$

The joint distribution density function and the marginal probability density functions can be obtained as:

$$\begin{cases} p(x_1, x_2) = \begin{cases} \tilde{C} exp\left[-\frac{x_1^2}{2\sigma_{x_1}^2} - \frac{x_2^2}{2\sigma_{x_2}^2} - \frac{2\eta(x_1 - x_2 - d)^{\frac{3}{2}}}{5\omega_1^2 \sigma_{x_1}^2}\right] \\ \quad when \quad x_1 - x_2 - d \geq 0 \\ \tilde{C} exp\left[-\frac{x_1^2}{2\sigma_{x_1}^2} - \frac{x_2^2}{2\sigma_{x_2}^2}\right] \quad else \end{cases} \\ p(x_1) = \int_{-\infty}^{\infty} p(x_1, x_2) dx_2 \\ p(x_2) = \int_{-\infty}^{\infty} p(x_1, x_2) dx_1 \\ p(v_1) = \frac{1}{\sigma_{v_1}\sqrt{2\pi}} exp\left(-\frac{v_1^2}{2\sigma_{v_1}^2}\right) \\ p(v_2) = \frac{1}{\sigma_{v_2}\sqrt{2\pi}} exp\left(-\frac{v_2^2}{2\sigma_{v_2}^2}\right) \end{cases} \tag{12}$$

where $\tilde{C}$ is the integration constant and can be obtained by

$$\int_{-\infty}^{\infty}\int_{-\infty}^{\infty} p(x_1, x_2) dx_1 dx_2 = 1 \tag{13}$$

It should be noted that the closed form expression can be obtained only under the assumptions of (1) (displacements and velocities are statistically independent) and (2) (the exciting strength ratio is equal to the damping and frequency ratio of two systems). Due to the assumptions, it has certain limitations when applied to explain the impact interactions on the responses of the vibro-impact system. However, it still provides useful insights into the impact interaction between the two vibration systems [30]. In this study, we will find out these limitations and the applicability of the analytical solution.

3. Numerical Analysis

3.1 The Time-domain Simulation

For simplicity, we use the bounded noise instead of the white noise Gaussian processes [31]. According to the work by Shinozuka [31], each physical realization of $\xi(t)$ can be approximated by the following triangle series expansion:

$$\begin{cases} \xi(t) \approx \sum_{k=1}^{N} A\cos(2\pi f_k t + \phi_k) \qquad N \longrightarrow \infty \\ A = \sqrt{2S_f \Delta f}; \ f_k \in [f_a, f_b]; \ \Delta f = \frac{f_b - f_a}{N} \\ \{\phi_k | k = 1,2,\ldots,N\} \sim U[0,2\pi] \end{cases} \tag{14}$$

where S_f is the one-sided power spectrum density(PSD) of the preset bounded noise, f_k are independent and nonnegative frequency over the interval $[f_a, f_b]$, Δf is the frequency increment and N is a fixed positive integer, random phase $\{\phi_k | k = 1,2,\ldots,N\}$ are uniformly distributed over the interval $[0,2\pi]$. Numerical results show that the physical realization generated by Eqs.(14) is almost stationary and ergodic when positive integer N is large enough[31]. To generate an ergodic physical realization, N is set to be large enough, say 50000. In general, we set $f_a = 0, f_b = 500$.

Assuming $\dot{x}_i = v_i$, Eqs. (1) can be replaced by the following equations:

$$\begin{cases} \dot{x}_1 = v_1 \\ \dot{v}_1 = -2\zeta_1\omega_1\dot{x}_1 - \omega_1^2 x_1 - \eta \cdot g(x_1, x_2) + \xi_1(t) \\ \dot{x}_2 = v_2 \\ \dot{v}_2 = -2\zeta_2\omega_2\dot{x}_2 - \omega_2^2 x_2 + \eta \cdot g(x_1, x_2) + \xi_2(t) \end{cases} \tag{15}$$

By using the simulations given in Eqs.(14), Eqs.(15) can be easily solved through numerical algorithms. To improve the computation precision, we choose the fourth-order Runge–Kutta algorithm with time step $\Delta t = 0.001s$, and for the purpose for making each system be stable ,the total time t is set to be 100s, then we can get a set of numerical solution (x_1, x_2, v_1, v_2) with 4×10^6 samples to provide a simulated PDF solution.

According to the theoretical analysis, under the assumptions (2), i.e. $\frac{S_1}{S_2} = \frac{\zeta_1\omega_1}{\zeta_2\omega_2}$, we can get the analytical solution of Eqs.(12). In order to exam the effectiveness of the numerical solution, we firstly set a group of parameters which satisfy Eq.(8) e.g. $\omega_1 = 32\pi$, $\omega_2 = 2\pi$, $\zeta_1 = \zeta_2 = 0.1, S_1 = 16, S_2 = 1, \eta = 10000, d = 0.05$. Figure 2 shows a comparison of the marginal PDFs of displacements and velocities between the numerical and the analytical solutions.

The blue curve shows the PDFs calculated by numerical method; the red dash line shows the PDFs calculated by analytical method; the green point curve shows the absolute errors of the PDFs. As we can see from Figure 2, the PDFs of displacement and velocity of System 1 obtained from the two methods agree well as seen by the almost zero error; However, obvious discrepancies can be seen from Figure 2(c) and (d) for System 2. When N is set to be 50000 in the simulation, there is a little fluctuations in the System 2. This phenomenon can be still observed when a much larger number of N is used. Nevertheless, the simulation of this study is acceptable on obtaining the approximate PDFs of the displacement and velocity responses of the system.

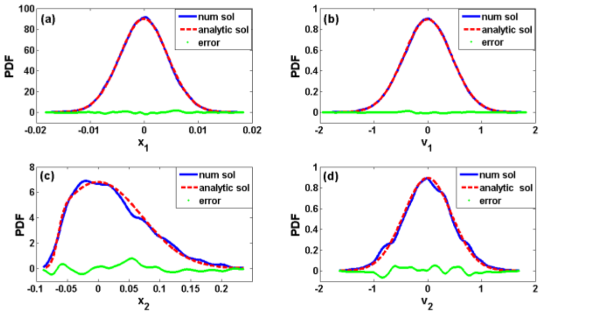

Figure 2. Comparisons of the PDFs: (a) displacement and (b) velocity of System 1; (c)displacement and (d)velocity of System 2.

3.2 The comparisons of the PDFs by using two methods

For the case In Figure 2, we have, $\overline{\omega} = \frac{\omega_1}{\omega_2} = 16$, $\overline{\zeta} = \frac{\zeta_1}{\zeta_2} = 1$, $\overline{S} = \frac{S_1}{S_2} = 16$, then $\frac{\overline{S}}{\overline{\zeta}\cdot\overline{\omega}} = 1$, which means the assumption (2) is satisfied. The PDFs of displacements and velocities responses of systems obtained from the two methods are almost the same as expected. Then, we adjust the value of ω_1 to calculate the PDFs of displacements and velocities responses for each system. As ω_1 changes, the assumption (2) is no longer satisfied. Therefore, the analytical solution may be not accurate anymore, so we need to know the deviation between the analytical solution and the numerical solution. Figure 3 and Figure 4 show the comparisons of the PDFs of the displacement and velocity responses of the systems with different ω_1 by using the two methods.

As we can see from Figure 3(a), $\overline{\omega} = 12$, $\frac{\overline{S}}{\overline{\zeta}\cdot\overline{\omega}} = 1.33$, the PDFs of System 1 coincide with those of System 2. In Figure 3(b), $\overline{\omega} = 8$, $\frac{\overline{S}}{\overline{\zeta}\cdot\overline{\omega}} = 2$, the PDFs of the displacement of velocity of System 1 calculated analytically still agree well with those from numerical simulations. In the contrast, the fluctuations in System 2 are more obvious; in Figure 3(c), when $\overline{\omega} = 4$, $\frac{\overline{S}}{\overline{\zeta}\cdot\overline{\omega}} = 4$, the PDFs of the System 1 still make good agreement, but there is a large discrepancy between the PDFs of System 2; in the Figure 3(d), $\overline{\omega} = 1$, the PDFs of both systems exhibit large derivations; in this case, $\frac{\overline{S}}{\overline{\zeta}\cdot\overline{\omega}} = 16 \gg 1$, that means the Eq.(9) is not satisfied anymore, so the exact analytical solution presents a great difference with the numerical solution . On the contrary, as we can see in Figure 4, even when ω_1 becomes much larger than ω_2, $\frac{\overline{S}}{\overline{\zeta}\cdot\overline{\omega}} < 1$, the PDFs of both methods agree well.

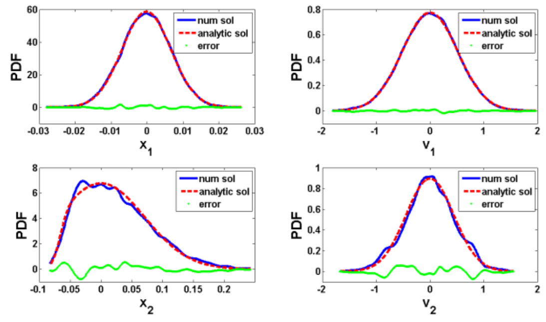

(a)$\omega_1 = 24\pi, \omega_2 = 2\pi, \overline{\omega} = 12$

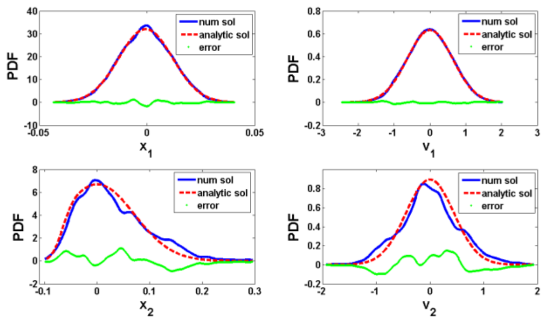

(b) $\omega_1 = 16\pi, \omega_2 = 2\pi, \overline{\omega} = 8$

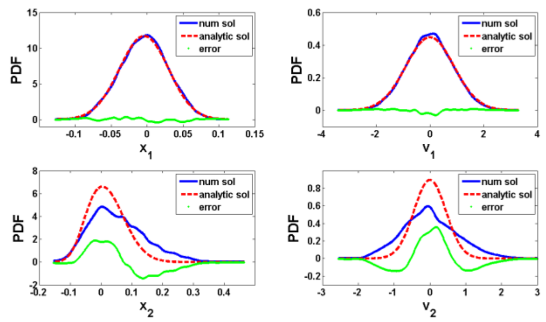

(c) $\omega_1 = 8\pi, \omega_2 = 2\pi, \overline{\omega} = 4$

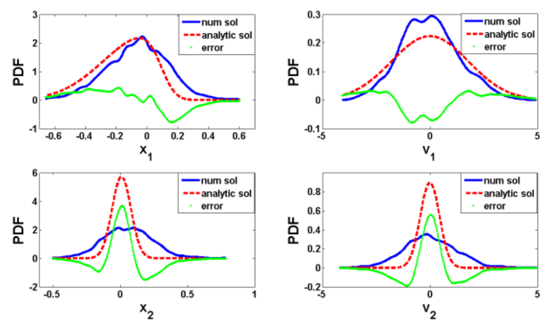

(d) $\omega_1 = 2\pi, \omega_2 = 2\pi, \overline{\omega} = 1$

Figure 3. PDFs of the responses of the systems ($\overline{\omega} = 12,8,4,1$).

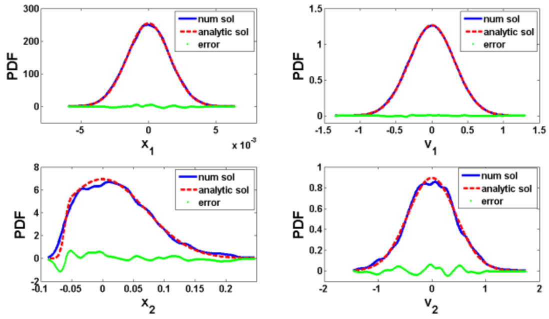

(a)$\omega_1 = 64\pi, \omega_2 = 2\pi, \overline{\omega} = 32$

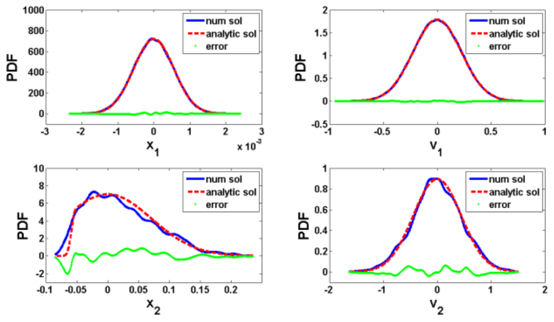

(b) $\omega_1 = 128\pi, \omega_2 = 2\pi, \overline{\omega} = 64$

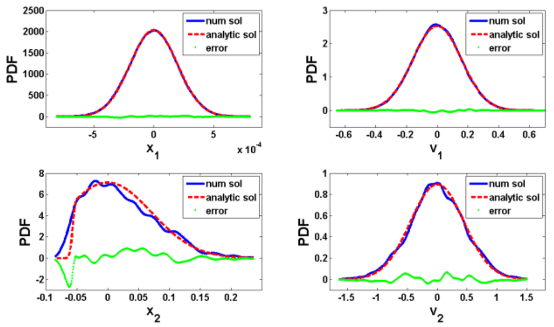

(c) $\omega_1 = 256\pi, \omega_2 = 2\pi, \overline{\omega} = 128$

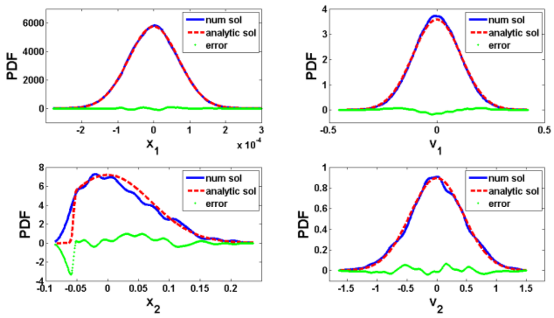

(d) $\omega_1 = 512\pi, \omega_2 = 2\pi, \overline{\omega} = 256$

Figure 4. PDFs of the responses of the systems ($\overline{\omega} = 32,64,128,256$)

3.3 Stochastic response analysis

In the study by Jing and Young [30], a parameter k_{12} is introduced to represent the square root of the stiffness ratio of each system and it can be derived as:

$$k_{12} = \sqrt{\frac{k_1}{k_2}} = \frac{\omega_1}{\omega_2} = \overline{\omega} = \frac{\overline{S}}{\overline{\zeta}} \cdot \frac{DV_2}{DV_1} = \sqrt{\frac{\overline{S}}{\overline{\zeta} \cdot \overline{\omega}} \cdot \frac{DX_2}{DX_1}} \qquad (16)$$

where $DV_i = \sigma_{v_i}^2 = \frac{\pi S_i}{2\zeta_i\omega_i}$ (in the numerical solution, we use one-sided PSD random excitations instead of the white noise Gaussian processes, so we have $DV_i = \sigma_{v_i}^2 = \frac{\pi S_i}{8\zeta_i\omega_i}$) represent the mean square velocity responses of the corresponding linear systems, and $DX_i = \sigma_{x_i}^2 = \frac{\pi S_i}{2\zeta_i\omega_i^3}$ (in the numerical solution, $DX_i = \sigma_{x_i}^2 = \frac{\pi S_i}{8\zeta_i\omega_i^3}$) represent the mean square displacement responses. According to the Eq.(16), we can define:

$$C_{DV} = \frac{DV_1}{DV_2} = \frac{\overline{S}}{\overline{\zeta} \cdot \overline{\omega}} \;\; ; \;\; C_{DX} = \frac{DX_1}{DX_2} = \frac{\overline{S}}{\overline{\zeta} \cdot \overline{\omega}^3} \qquad (17)$$

which represent the mean square responses ratio of the corresponding linear systems. It can be seen that, only when the assumption (2) is satisfied, $k_{12} = \overline{\omega} = \sqrt{\frac{DX_2}{DX_1}} = \sqrt{\frac{1}{C_{DX}}} = \frac{\sigma_{x_2}}{\sigma_{x_1}}$ which is the same as which given by Jing and Young [30]. It's worth noting that, C_{DV} represents the satisfaction of the assumption 2.

It is noted that, according to the Eq.(12), the velocity distributions of v_1 and v_2 are decoupled and Gaussian, so the mean square velocity responses of the vibro-impact systems are equal to those of the linear systems. But the displacement distributions of x_1 and x_2 are coupled due to the impact interactions, which is governed by $g(x_1, x_2)$. And the mean square displacement responses of the vibro-impact system can be obtained as

$$D_{x_i'} = \int_{-\infty}^{\infty} x_i^2 \cdot p(x_i) dx_i \;,\;\; i = 1,2 \qquad (18)$$

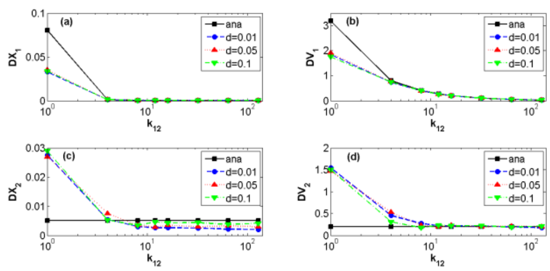

Figure 5. Mean square responses with different clearance: (a) displacement and (b) velocity responses of the System 1; (c) displacement and (d) velocity responses of the System 2.

It is found that the mean square responses calculated by the two methods are significantly different, which can be observed from Figure 5. Figure 5 (a) and (c) show the differences of the mean square displacement responses. As we can see, when $\overline{\omega} = 1, C_{DV} = 16 \gg 1$, the mean square displacement responses have great differences: the analysis results of the vibro-impact systems are greater than the numerical results for System 1; and the analysis results of the linear systems (the black square line) are the greatest. In the contrast, the numerical results are the greatest for System 2. This phenomenon is due to the strong impact interaction, which reduces the mean square displacement responses of System 1 while increases the mean square responses of System 2. As $\overline{\omega}$ increases and C_{DV} decreases, the stiffness of System 1 becomes larger, these differences vanish quickly: when $\overline{\omega} \geq 8$, the analysis results and the numerical results are almost the same; but for System 2, the analysis results of corresponding linear systems are always larger than the results of vibro-impact systems.

Figure 5 (b) and (d) show the differences of the mean square velocity responses. In the theoretical analysis, the velocity distributions of v_1 and v_2 are decoupled and Gaussian. However, in the numerical analysis, though the velocity distributions of v_1 and v_2 are still Gaussian, the mean square responses differ with the results from theoretical analysis. Similar to the mean square displacement responses, when $\overline{\omega} = 1, C_{DV} = 16$, the analytical results are greater for System 1, while the numerical results are greater for System 2. As $\overline{\omega}$ increases and C_{DV} decreases, these differences vanish quickly: for System 1, when $\overline{\omega} \geq 8, C_{DV} \leq 2$, the analysis results and the numerical results are almost the same; but for System 2, the numerical results approximate to the analysis results until $\overline{\omega} \geq 12, C_{DV} \leq 1.33$. The results suggest that the impact interaction does not only influence the displacement distributions but also the velocity distributions.

The influence of clearance d on the system response is also worth attention. The mean square responses of the systems with different clearance are also shown in Figure 5. From Figure 5 (a) and (b) we can find that, changing clearance will have little impact on the mean square responses of the system 1; from Figure 5(c) and (d) we can find that, changing clearance will have some influences on the mean square responses of the system 2: the mean square displacement responses of System 2 with a clearance $d = 0.1$ are slightly larger than which with a clearance $d = 0.05$ and $d = 0.01$; on the contrary, the mean square velocity responses of System 2 with a clearance $d = 0.1$ are slightly smaller than which with a clearance $d = 0.05$ and $d = 0.01$.

The mean square responses ratio calculated by the two methods also show great differences, which can be observed from Figure 6. As we can see from Figure 6, the relationship between the mean square responses ratio of the linear systems and $\overline{\omega}$ is linear in log-log scale. The mean square responses ratio of the vibro-impact systems calculated by the analysis method is in a good agreement with that of the linear systems. However, for the mean displacement square responses ratio, when $\overline{\omega} = 1, C_{DV} = 16$, the numerical results of the vibro-impact systems are much smaller than the analysis results; for the mean velocity square responses ratio, the numerical results are smaller than the analysis results when $\overline{\omega} \leq 8$; especially when $\overline{\omega} = 1, C_{DV} = 16$, the numerical results are much smaller than the analysis results. These results suggest that the relationship between the mean square responses ratio of the vibro-impact systems and $\overline{\omega}$ is nonlinear in log-log scale. Changing clearance will have little impact on the mean square responses ratio of the systems.

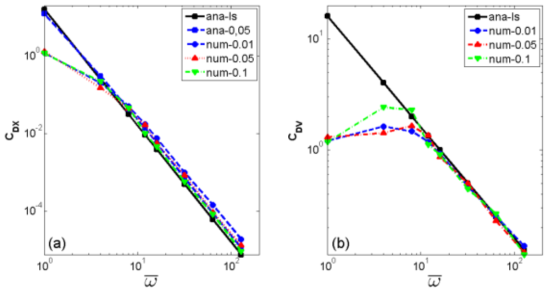

Figure 6. Mean square responses ratio with different clearance (log log-scale): (a) mean displacement square responses ratio mean; (b) velocity square responses ratio.

The contact ratio is defined as the summation of the time intervals while contact is maintained divided by the total time. The variations of the contact ratio with $\overline{\omega}$ are shown in Figure 7. As we can see in Figure 7, when $\overline{\omega}$ is constant, the smaller the clearance d, the greater the contact ratio. When $d = 0.01$, the contact ratio increases rapidly with increasing of the clearance at first, then it increases smoothly and become stable when $\overline{\omega} > 16$; in contrast, when $d = 0.1$, the contact ratio decreases rapidly to the minimum when $\overline{\omega} = 8$, then it increases smoothly and becomes stable; when $d = 0.05$, the contact ratio have a jump value while $\overline{\omega} = 4$, besides which the rest remains steady.

The maximum impact force response of the systems is also worth attention. Figure 8 shows the variations of the maximum impact force with $\overline{\omega}$. As we can see in Figure 8, when $\overline{\omega}$ is constant, the smaller the clearance d, the greater the maximum impact force. When $\overline{\omega} = 1$, the maximum impact force reaches to the peak value; with the increase of $\overline{\omega}$, the maximum impact force decreases rapidly at first, then it decreases smoothly and becomes stable.

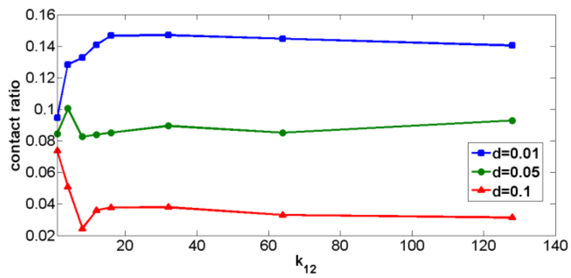

Figure 7. The variations of the contact ratio with $\overline{\omega}$.

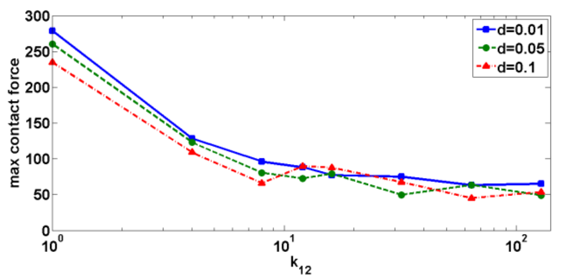

Figure 8. The variations of the maximum impact force with $\overline{\omega}$.

4. Conclusions

In this paper, the analytical solution of the vibro-impact systems under random excitation is obtained using the classical FPK method under the assumptions of (1) (displacements and velocities are statistically independent) and (2) (the exciting strength ratio is equal to the damping and frequency ratio of two single-degree-of-freedom vibration systems). The Hertz contact model is used to describe the contact between two single-degree-of-freedom vibration systems. The numerical solutions of the vibro-impact system are obtained by the IDFT and the Runge-Kutta method.

Through the comparisons of the PDFs of the displacement and velocity responses of the systems calculated by using the two methods, the deviation between the analytical solution and the numerical solution is studied. The mean square responses are also calculated. And the mean square responses ratio of the systems is introduced to represents the satisfaction of the assumption (2): when $C_{DV} = 1$, the assumption (2) is satisfied. When the frequency ratio $\overline{\omega} \geq 12$, the mean square responses ratio of the corresponding linear systems $C_{DV} \leq 1.33$, the PDFs calculated by the two methods are in good agreement; C_{DV} increases as $\overline{\omega}$ decreases, and the differences between the PDFs from the two methods become significant. The displacement distribution and velocity distribution are significantly affected by the impact interaction: when the impact interaction is strong, the mean square responses show a great difference. It is found that, the relationship between the mean square responses ratio of the linear systems and $\overline{\omega}$ is linear in log-log scale; while that of the vibro-impact systems is nonlinear.

Finally, the influence of clearance on the responses of the systems is studied. Changing clearance will have little impact on the mean square responses of the systems. When $\overline{\omega}$ is constant, the smaller the clearance d, the greater the contact ratio and the maximum impact force.

Acknowledgements

The financial support from the Program For Scientific Research Start-Up Funds Of Guangdong Ocean University (R19020) and the Science and Technology Project of Zhanjiang City (2020B01465) to this work is gratefully acknowledged.

Conflict of Interest Statement

The authors declare that the research was conducted in the absence of any commercial or financial relationships that could be construed as a potential conflict of interest.

References

[1] Babitsky, V.I., Theory of Vibro-impact Systems, Nauka, Moscow, (1978).

[2] Kobrinski, A.E., Dynamic of Mechanisms with Elastic Connection and Impact System, English Translation: R.Lennox-Napier, Iliffe, London, (1969).

[3] Wolf, J.P., Soil-Structure-Interaction Analysis in Time Domain, Nuclear Engineering & Design, 111 (1989) 381–393.

[4] Shaw, S.W. and Holmes, P.J., A periodically forced piece wise linear oscilinear, Journal of Sound and Vibration, 90 (1983) 129–155.

[5] Luo, G.W. and Xie, J. H., Hopf-bifurcation of a two-degree-of-freedom vibro-impact system”, Journal of Sound and Vibration, 213 (1998) 391–408.

[6] Luo, G.W. and Xie, J. H., Bifurcations and chaos in a system with impacts, Physica D, 148 (2001) 183-200.

[7] Luo, G.W. and Xie, J. H., Stability of periodic motion, bifurcations and chaos of a two-degree-of-freedom vibratory system with symmertical rigid stops, Journal of Sound and Vibration, 273 (2004) 543–568.

[8] Dimentberg, M.F. and Iourtchenko, D.V., Random vibration with impact: a review, Nonlinear Dynamics, 36 (2004) 229–254.

[9] Goldsmith, W., Impact: The Theory and Physical Behavior of Colliding Solids, Edward Arnold, London, (1960).

[10] Caughey, T.K., Derivation and application of the Fokker-Planck equation to discrete nonlinear dynamic systems subjected to white random excitation, Journal of the Acoustical Society of America, 35 (1963) 1683–1692.

[11] Caughey, T.K. and Ma, F., The exact steady-state solution of a class of non-linear stochastic systems, International Journal of Non-Linear Mechanics, 17 137–142 (1982).

[12] Dimentberg, M.F. and Menyailov, A.I., Response of a single-mass vibro-impact system to white-noise random excitation, Zamm Journal of Applied Mathematics and Mechanics, 59 (1979) 709–716.

[13] Dimentberg, M.F., An exact solution to a certain non-linear random vibration problem, International Journal of Non-Linear Mechanics, 17 (1982) 231–236.

[14] Jing, H.S. and Sheu, K.C., Exact stationary solutions of the random response of a single-degree-of-freedom vibro-impact system”, Journal of Sound and Vibration, 141 (1990) 363–373.

[15] Jing, H.S. and Young, M., Random response of a single-degree-of-freedom vibro-impact system with clearance, Earthquake Engineering and Structural Dynamics, 19 (1990) 789–798.

[16] Wang, R. and Zhang, Z., Exact stationary solutions of the Fokker-Planck equation for nonlinear oscillators under stochastic parametric and external excitations, Nonlinearity, 13 (2000) 907–920.

[17] Zhuravlev, V.F., A method for analyzing vibration-impact systems by means of special functions, Mechanics of Solids, 11 (1976) 23–27.

[18] Huang, Z.L. and Zhu, W.Q., Exact stationary solutions of stochastically and harmonically excited and dissipated integrable hamiltonian systems, Journal of Sound and Vibration, 230 (2000) 709–720.

[19] Huang, Z.L., Liu, Z.H. and Zhu, W.Q., Stationary response of multi-degree-of freedom vibro-impact systems under white noise excitations, Journal of Sound and Vibration, 275 (2004) 223–240.

[20] Feng, J.Q., Xu, W. and Rong, H.W., Stochastic responses of Duffing-Van der Pol vibro-impact system under additive and multiplicative random excitations, International Journal of Non-Linear Mechanics, 44 (2009) 51–57.

[21] Rong, H.W., Wang, X., Xu, W. and Fang, T., Resonant response of a non-linear vibro-impact system to combined deterministic harmonic and random excitations, International Journal of Non-Linear Mechanics, 45 (2010) 474–481.

[22] Er, G.K., An improved closure method for analysis of nonlinear stochastic systems, Nonlinear Dynamics, 17 285–297 (1998).

[23] Zhu, H.T., Er, G.K., Iu, V.P. and Kou, K.P., EPC procedure for PDF solution of nonlinear oscillators excited by Poisson white noise, International Journal of Non-Linear Mechanics, 44 (2009) 304-310.

[24] Zhu, H.T., Stochastic response of vibro-impact Duffing oscillators under external and parametric Gaussian white noises, Journal of Sound and Vibration, 333 (2014) 954–961.
[25] Pantelides, C.P. and Ma, X., Linear and nonlinear pounding of structural systems, Computers and Structures, 66 (1998) 79–92.
[26] Chau, K.T. and Wei, X.X., Pounding of structures modelled as non-linear impacts of two oscillators, Earthquake Engineering and Structural Dynamics, 30 (2001) 633–651.
[27] Jankowski, R., Non-linear viscoelastic modelling of earthquake-induced structural pounding, Earthquake Engineering and Structural Dynamics, 34 (2005) 595–611.
[28] Jankowski, R., Analytical expression between the impact damping ratio and the coefficient of restitution in the non-linear viscoelastic model of structural pounding, Earthquake Engineering and Structural Dynamics, 35 (2006) 517–24.
[29] Jankowski, R., Pounding force response spectrum under earthquake excitation, Engineering Structures, 28 (2006) 1149–1161.
[30] Jing, H.S. and Young, M., Impact interactions between two vibration systems under random excitation, Earthquake Engineering and Structural Dynamics, 20 (1991) 667–681.
[31] Shinozuka, M., Digital simulation of random processes and its applications, Journal of Sound and Vibration, 25 (1972) 111–128.
[32] Lin, Y.K. and Cai, G.Q., Probabilistic Structural Dynamics-Advanced Theory and Applications, McGraw-Hill, Singapore,(1995).
[33] Rahimi, S., Carver, N., Petry, F. (2005). A Multi-Agent Architecture for Distributed Domain-Specific Information Integration. In: Ladner, R., Petry, F.E. (eds) Net-Centric Approaches to Intelligence and National Security. Springer, Boston, MA. https://doi.org/10.1007/0-387-26176-1_7
[34] S. Neupane *et al*., Explainable Intrusion Detection Systems (X-IDS): A Survey of Current Methods, Challenges, and Opportunities, *IEEE Access*, 10 (2022) 112392–112415, doi: 10.1109/ACCESS.2022.3216617.
[35] S. B. Ramezani et al., A novel compartmental model to capture the nonlinear trend of COVID-19, Computers in Biology and Medicine, 134 (2021) 104421, https://doi.org/10.1016/j.compbiomed.2021.104421.
[36] T. S. Tabrizi et al., Towards a patient satisfaction based hospital recommendation system, *2016 International Joint Conference on Neural Networks (IJCNN)*, Vancouver, BC, Canada, 2016, pp. 131–138, doi: 10.1109/IJCNN.2016.7727190.
[37] Khorasani, E.S., Patel, P., Rahimi, S. *et al.* An inference engine toolkit for computing with words. *J Ambient Intell Human Comput* **4**, 451–470 (2013). https://doi.org/10.1007/s12652-012-0137-8
[38] N. Marhamati et al., Integration of Z-numbers and Bayesian decision theory: A hybrid approach to decision making under uncertainty and imprecision, Applied Soft Computing, 72 (2018) 273–290, https://doi.org/10.1016/j.asoc.2018.07.053.